International Journal of Applied Mathematics
Volume 38 No. 7s, 2025
ISSN: 1311-1728 (printed version); ISSN: 1314-8060 (on-line version)

IMPROVING UNDERWATER SEMANTIC SEGMENTATION VIA ADAPTIVE FREQUENCY-AWARE ENHANCEMENT AND THE SEGMENT ANYTHING MODEL

Abhisheka Thumbesara Eshwara[1, 2], Basavaraj Ningappa Jagadale[3], Madhuri Gurram Ramesh[4], Chandrakantha Tholalemane Satyanarayana[5]

[1]Department of Electronics, Research Scholar, Jnanasahyadri, Kuvempu University, Shankaraghatta, Shivamogga, Karnataka, India

[2]Department of Electronics, Junior Technical Officer, All India Institute of Speech and Hearing, Mysuru, Karnataka, India

[3]Department of Electronics, Faculty in Electronics, Jnanasahyadri, Kuvempu University, Shankaraghatta, Shivamogga, Karnataka, India

[4]Department of Electronics, Faculty in Electronics, Jnanasahyadri, Kuvempu University, Shankaraghatta, Shivamogga, Karnataka, India

[5] Department of Electronics, Research Scholar, Jnanasahyadri, Kuvempu University, Shankaraghatta, Shivamogga, Karnataka, India

Abstract

The segmentation of underwater images is a challenging task in computer vision and marine research due to factors such as low contrast, non-uniform illumination, and color distortion. Despite advances in deep learning, segmentation performance often remains suboptimal. Effective preprocessing of underwater images is therefore essential for improved accuracy. This study proposes a hybrid deep learning framework that combines image enhancement with robust segmentation. Low- and high-frequency components of the image are filtered using Bilateral and Difference-of-Gaussian filters, while an adaptive variational strategy prevents oversaturation and over-enhancement of color and contrast. The enhancement process reduces noise, optimizes contrast, and recovers critical features, facilitating more accurate segmentation. The deep learning component leverages a robust architecture and extensive datasets to further improve segmentation performance. Evaluation using quantitative metrics and visual results demonstrates that the proposed approach significantly enhances underwater image segmentation, benefiting applications in marine exploration, monitoring, and research.

KEY WORDS AND PHRASES: Image enhancement, Deep learning, Segment anything model, Underwater image segmentation, Image denoising.

1. Introduction

Underwater image segmentation is a challenging yet essential task in computer vision, supporting diverse applications such as marine biology, underwater robotics, archaeology, and environmental monitoring [1]– [4]. Unlike standard images, underwater visuals are often degraded by low contrast, non-uniform illumination, color distortion, and scattering effects caused by absorption and turbidity. These degradations significantly reduce the accuracy of segmentation methods [1], [2].

Deep learning-based semantic segmentation models such as U-Net, SegNet, and the Segment Anything Model (SAM) have achieved state-of-the-art performance in many domains [5]– [8]. However, their direct application to underwater datasets remains limited due to two major challenges: (i) poor visual quality of underwater images, and (ii) scarcity of large, annotated datasets specific to underwater environments [2], [7], [9]. Because most deep models are highly data-driven, their generalizability is affected when domain shifts occur in underwater imagery.

To address these challenges, image enhancement techniques have been widely explored as a preprocessing step to improve the visibility and quality of underwater images prior to segmentation. Classical methods such as Histogram Equalization, Contrast Limited Adaptive Histogram Equalization (CLAHE), Unsupervised Color Correction, and Hybrid Fusion approaches [1], [10]–[13] have been proposed to mitigate visibility degradation. However, not all enhancement strategies are equally effective in preserving structural and semantic information that is critical for segmentation, and relatively few studies have systematically examined how specific enhancement techniques impact segmentation accuracy.

In this study, we propose a hybrid framework that integrates Adaptive Color and Contrast Enhancement with Denoising (ACCE-D) and the Segment Anything Model (SAM) [8] for robust underwater image segmentation. The ACCE-D enhancement stage employs Difference of Gaussian (DoG) and Bilateral filtering to separate and refine low- and high-frequency components, followed by an adaptive variational strategy in the HSI color space to suppress noise and prevent over-enhancement. The enhanced images are then processed by SAM, a transformer-based segmentation model pre-trained on 11 million images and 1.1 billion masks. With its zero-shot, prompt-based capability, SAM is particularly suited to segmentation tasks where annotated underwater data is scarce.

By combining domain-specific enhancement with a large-scale foundation segmentation model, our approach preserves both structural and semantic features in underwater imagery, enabling more accurate segmentation even under severe degradations.

The key contributions of this work are as follows:

- We present a novel integration of the ACCE-D enhancement framework with the SAM segmentation model to improve underwater image segmentation.
- We conduct comparative evaluations against widely used enhancement methods and deep learning-based segmentation models to benchmark the effectiveness of the proposed approach.
- We perform an ablation study to quantify the role of each stage in the enhancement pipeline on final segmentation accuracy.
- We provide experimental validation on multiple underwater datasets using standard evaluation metrics such as Intersection over Union (IoU), Dice Similarity Coefficient (DSC), and Hausdorff Distance at the 95th Percentile (HD95).

The rest of this paper is organized as follows: Section 2 reviews existing work on underwater image enhancement, segmentation techniques, and hybrid models. Section 3 describes the proposed methodology, including ACCE-D enhancement, SAM-based segmentation, and evaluation design. Section 4 details the datasets used in this study. Section 5 explains the segmentation model architecture. Section 6 presents results and discussion, including visual and quantitative analysis, comparisons, and ablation studies. Finally, Section 7 concludes the paper and outlines future research directions.

2. Related Work

2.1 Underwater Image Enhancement Techniques

Underwater images often suffer from poor visibility, low contrast, and color distortions due to light absorption and scattering. Several preprocessing methods have been developed to address these challenges. Histogram-based methods like CLAHE [14] perform local histogram equalization in contextual regions, enhancing contrast and visibility. Similarly, the Unsupervised Colour Correction Method (UCM) [15] improves color balance by adjusting red and blue channels through histogram equalization.

Color model transformations are also popular. The Hue Saturation Intensity (HSI) model and CIE-Lab space have been used to address illumination inconsistency and perform contrast correction. Relative Global Histogram Stretching (RGHS) [16] enhances shallow-water images through adaptive contrast stretching and color normalization, while Histogram Equalization (HE) [17] improves image quality by adjusting pixel intensity distributions.

Other works have employed model-based techniques. The Integrated Colour Model (ICM) [18] converts RGB values to HSI to manage color distortion. Histogram modification [19] using Rayleigh distributions and Von Kries adaptation has also been applied to enhance contrast and correct color shifts. The gamma correction as a preprocessing technique to enhance image visibility and contrast. Their results demonstrated improved segmentation accuracy, especially in low-light or low-contrast scenarios [20]. Fusion-based approaches combine multiple enhancement cues. The classic fusion method [21] extracts image properties and merges them using a fusion framework. More recent work proposes Hybrid Fusion Modules (HFM) [22] that incorporate Nonlinear Colour Mapping, the Gray World Principle, and fuzzy logic for comprehensive enhancement of contrast, white balance, and visibility.

The ACCE-D [23], relevant to our study, combines DoG filters and bilateral filtering to extract high and low-frequency components. It employs a variational framework in the HSI space for controlled enhancement, while soft thresholding and Gaussian weights prevent over-enhancement and oversaturation. This method has shown promising results in balancing detail preservation and noise suppression. Wavelet-based techniques like the Weighted Wavelet Perception Fusion (WWPF) [24] address global and local contrast using entropy-driven strategies and attenuation maps, followed by inverse fusion for perceptual quality restoration.

2.2 Deep Learning Approaches for Segmentation

Deep learning has emerged as the state-of-the-art for image segmentation. Transformer-based architectures such as Vision Transformer (ViT) and MLP-Mixer [25] challenge traditional CNNs by modelling global dependencies using matrix operations and token mixing layers, achieving superior performance on large datasets. Among convolutional models, SegNet [26] stands out for its encoder-decoder structure utilizing VGG-16 layers. It uses max-pooling indices to preserve spatial resolution during up sampling, offering efficient semantic segmentation for dense prediction tasks.

Specific adaptations have been made for underwater image segmentation. For instance, SegNet was trained on a synthesized underwater dataset (ULTIR) [27], where Support Vector Machines were used for post-processing segmentation masks. Another method, MA-AttUNet [28], employed multi-level adversarial transfer learning to detect underwater dam cracks by transferring knowledge from a source domain to a low-data target domain. For instance, segmentation tasks like fish detection, Alshdaifat et al. [29] used ResNet-based models preceded by image enhancement. This approach extracted contextual information using ReNet layers, effectively segmenting underwater organisms despite degraded conditions.

2.3 Hybrid Approaches: Linking Enhancement and Segmentation

Despite extensive work in enhancement and segmentation as separate domains, relatively few studies explore their joint impact. Recent research highlights the growing importance of integrating underwater image enhancement with downstream tasks such as segmentation. For example, Deng et al. [30] introduced CFormer, a CNN–Transformer hybrid model, which improved segmentation and detection by using enhanced images as input. Similarly, Chen et al. [31] proposed a task-guided enhancement network, where feedback from a detection model steered the enhancement process, resulting in better downstream performance. Qian et al. [32] presented HA-Net, which combines traditional filters and deep networks to improve texture and edge clarity factors critical for segmentation.

While these works confirm the potential of enhancement-aware designs, few have explored their direct impact on segmentation performance using standardized models like SAM. Our work addresses this gap by evaluating how different enhancement methods—especially the proposed ACCE-D pipeline—affect the segmentation outcomes, isolating enhancement as a key variable in underwater image analysis. This helps to evaluate the effect of enhancement on segmentation performance. Compared to traditional enhancement pipelines (e.g., HE, ICM, fusion methods), ACCE-D is particularly suited for underwater contexts due to its frequency-aware decomposition and adaptive contrast mechanisms. Its integration with a general-purpose segmentation model like SAM demonstrates how domain-specific preprocessing can significantly elevate downstream segmentation outcomes — a relatively underexplored yet impactful research direction.

3. Methodology

The proposed method introduces a hybrid strategy for robust underwater image segmentation by combining an enhancement model (ACCE-D) with a transformer-based segmentation model (SAM). The pipeline operates in two stages: (i) image enhancement using ACCE-D and (ii) segmentation using a pre-trained SAM model (`sam_vit_h_4b8939.pth`). Figure 1 illustrates the overall workflow.

ISSN: 1311-1728 (printed version); ISSN: 1314-8060 (on-line version)

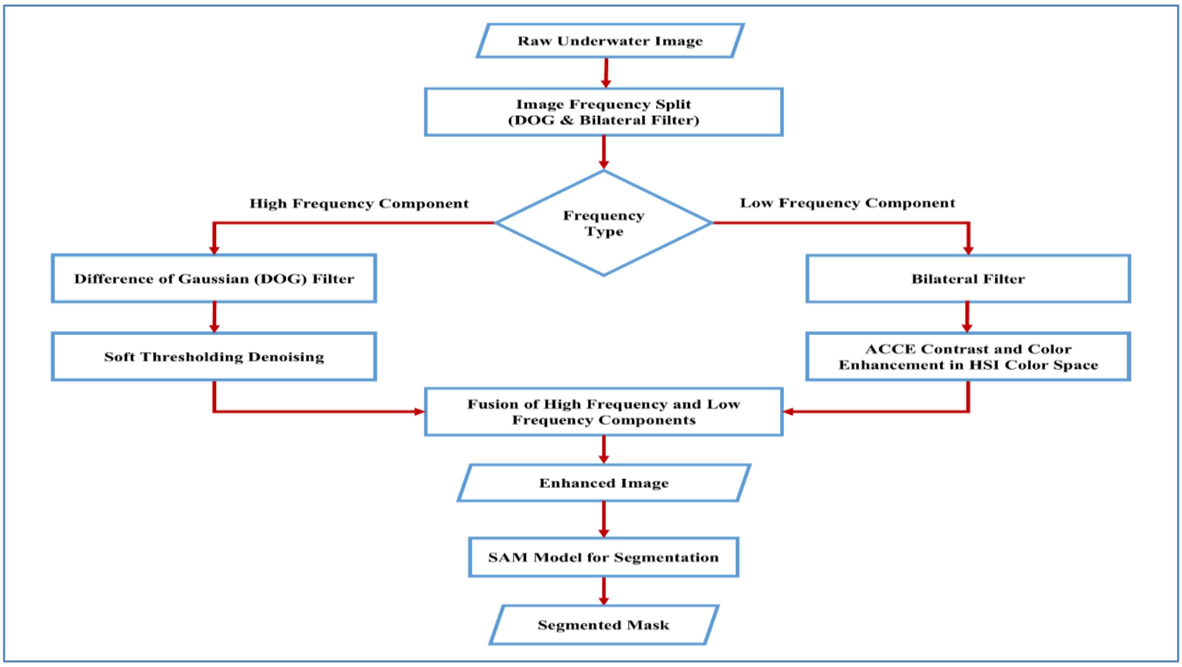

Figure 1. Flowchart of the proposed hybrid approach combining ACCE-D image enhancement and SAM segmentation.

3.1 Stage 1: Image Enhancement using ACCE-D

Underwater images are often degraded by turbidity, scattering, and color attenuation, which severely limit segmentation accuracy. To address this, we first apply Adaptive Color and Contrast Enhancement with Denoising (ACCE-D). The enhancement procedure is as follows:

1. Frequency Decomposition: The input RGB image is decomposed into high- and low-frequency components. Low-frequency components are extracted using bilateral filtering, which smooths textures while preserving edges. High-frequency components are processed using a Difference of Gaussian (DoG) filter combined with soft thresholding to suppress noise while retaining edge details.

2. Adaptive Variational Processing in HSI Color Space: The low-frequency image is converted into the HSI color space, and enhancement is applied to the intensity and saturation channels using an adaptive variational strategy. This correction restores color balance and prevents over-enhancement.

3. Fusion: The denoised high-frequency components and enhanced low-frequency components are fused to generate the final enhanced image.

The final enhanced image is generated by fusing both filtered components. This enhancement process is guided by an energy function E(I), defined as:

$$E(I) = \lambda \cdot \|\tilde{I}\_H - I\_H\|^2 + (1 - \lambda) \cdot \|\tilde{I}\_L - I\_L\|^2 + \alpha \cdot R(I)$$

Where:

- **E(I)**: Total energy of the enhanced image.
- **$\tilde{I}_H$, I_H**: Denoised and original high-frequency components.
- **$\tilde{I}_L$, I_L**: Enhanced and original low-frequency components.
- λ: Weighting factor between high- and low-frequency terms.

International Journal of Applied Mathematics
Volume 38 No. 7s, 2025
ISSN: 1311-1728 (printed version); ISSN: 1314-8060 (on-line version)

- **R(I)**: Optional regularization term (e.g., histogram similarity or total variation).
- **α**: Regularization weight.

3.2 Stage 2: Segmentation with SAM

The enhanced image is then passed to the Segment Anything Model (SAM) for segmentation. In this study, we use the ViT-H backbone checkpoint (`sam_vit_h_4b8939.pth`), which has been pre-trained on 11 million images and 1.1 billion masks. SAM is a prompt-based model capable of zero-shot segmentation across diverse domains, making it suitable for underwater imagery where labelled datasets are scarce.

We employ the Bounding Box prompt to specify the Region of Interest (ROI). The enhanced image is encoded using SAM's Vision Transformer (ViT), which generates image embeddings of size 256 × 64 × 64. A mask decoder, built on attention mechanisms and multilayer perceptrons (MLPs), outputs three candidate masks. The final mask is automatically selected based on maximum alignment with the object boundaries.

3.3 Evaluation Metrics

The performance of the proposed model is evaluated using standard segmentation metrics as given in the Table 1.

Table 1. Segmentation quality testing metrics and their formula

Quality Testing Metric	Formula
IoU	$\frac{TP}{TP+FN+FP}$
DSC	$\frac{2TP}{2TP+FN+FP}$
HD95	HD95(A,B)=max{P95($b \in B_{min}$‖a−b‖), P95 ($a \in A_{min}$‖b−a‖)}

Where:

- TP, FP, FN: True Positive, False Positive, and False Negative
- A, B: Boundary points of predicted and ground truth segmentations
- ||·||: Euclidean distance
- P95: 95th percentile, used to make HD95 robust to outliers

Unlike the standard Hausdorff Distance (HD), which uses the maximum distance and is highly sensitive to outliers, HD95 uses the 95th percentile of distances, providing a more stable and representative boundary discrepancy metric for segmentation evaluation.

International Journal of Applied Mathematics
Volume 38 No. 7s, 2025
ISSN: 1311-1728 (printed version); ISSN: 1314-8060 (on-line version)

3.4 Experimental Comparison

To validate the effectiveness of the proposed hybrid approach, the model was evaluated on various underwater images and benchmarked against several enhancement techniques—such as CLAHE, HE, ICM, UCM, Rayleigh Stretching, HFM, PDCE, and WWPF—as well as a range of segmentation models including U-Net [33], U-Net (ResNet) [34], U-Net (VGG) [35], SegNet [36], SUIMNet [37], BiSeNetV2 [38], PSPNet [39], UISS-Net [40], DeepLab [41], LEDNet [42], SAM2 [43], and EfficientSAM [44]. Segmentation performance was assessed using standard evaluation metrics to provide a comprehensive comparison.

The Figure 2 shows the comprehensive diagram of proposed model. The proposed deep learning model is a promptable segmentation model*, offering three types of prompts to select the ROI: Point, Bounded Box, and Text. In this model, the Bounding Box prompting method is selected, providing a clear spatial frame for the ROI and enabling the algorithm to precisely determine the target area [45].

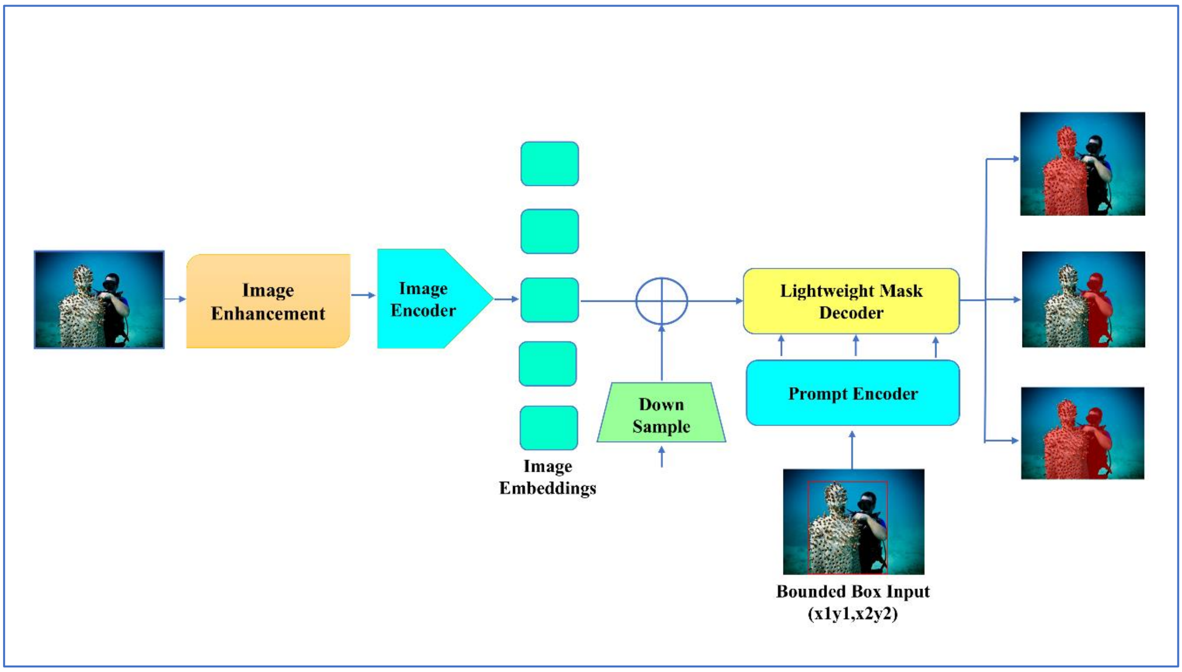

Figure 2. The hybridized deep learning model for underwater image segmentation.

** Conceptually, this model can run even without a prompt in segment everything mode, but it does not help to segment the ROI.*

4. Datasets

The effectiveness of the proposed method was evaluated on images that were significantly degraded by the challenging conditions of the underwater environment. To assess the model's generalizability, three different underwater datasets were employed: SUIM, NAUTEC UWI Real, and EUVP. In total, 50 degraded images were selected across these datasets to examine how enhancement influences segmentation performance.

International Journal of Applied Mathematics
Volume 38 No. 7s, 2025
ISSN: 1311-1728 (printed version); ISSN: 1314-8060 (on-line version)

The SUIM dataset is one of the most widely used benchmarks for underwater semantic segmentation. It contains more than 1,500 images across eight object categories, with pixel-level annotations. The dataset provides 110 test images and separate ground-truth masks for each object class, making it suitable for evaluating semantic segmentation models in diverse underwater scenarios.

The NAUTEC UWI Real dataset consists of 700 real-world underwater images collected from online sources. The dataset incorporates images captured under a variety of lighting conditions, water types, and depths, including both benthic and pelagic zones. It features imagery obtained with both natural and artificial illumination, providing a diverse test bed for segmentation in realistic conditions.

The EUVP dataset was originally developed for underwater image enhancement tasks and does not include ground-truth segmentation masks. To enable evaluation, ground-truth annotations were generated for a subset of selected EUVP images by manually delineating object boundaries using the ImageJ tool. The EUVP collection contains approximately 20,000 images, organized into paired and unpaired sets with varying perceptual quality. For this study, the most visually degraded examples were chosen to better assess the robustness of the proposed enhancement–segmentation pipeline.

5. Model Used For Segmentation

This study employs the SAM, a state-of-the-art vision transformer model designed for zero-shot segmentation [46]. SAM generalizes well to unseen images without additional training, making it suitable for underwater image analysis, where annotated datasets are limited. Figure 3 shows the segmentation capability of SAM on degraded underwater images by evaluating the segmented results using IoU and DSC metrics. The red color mask in the third column is the mask generated by SAM on the target area.

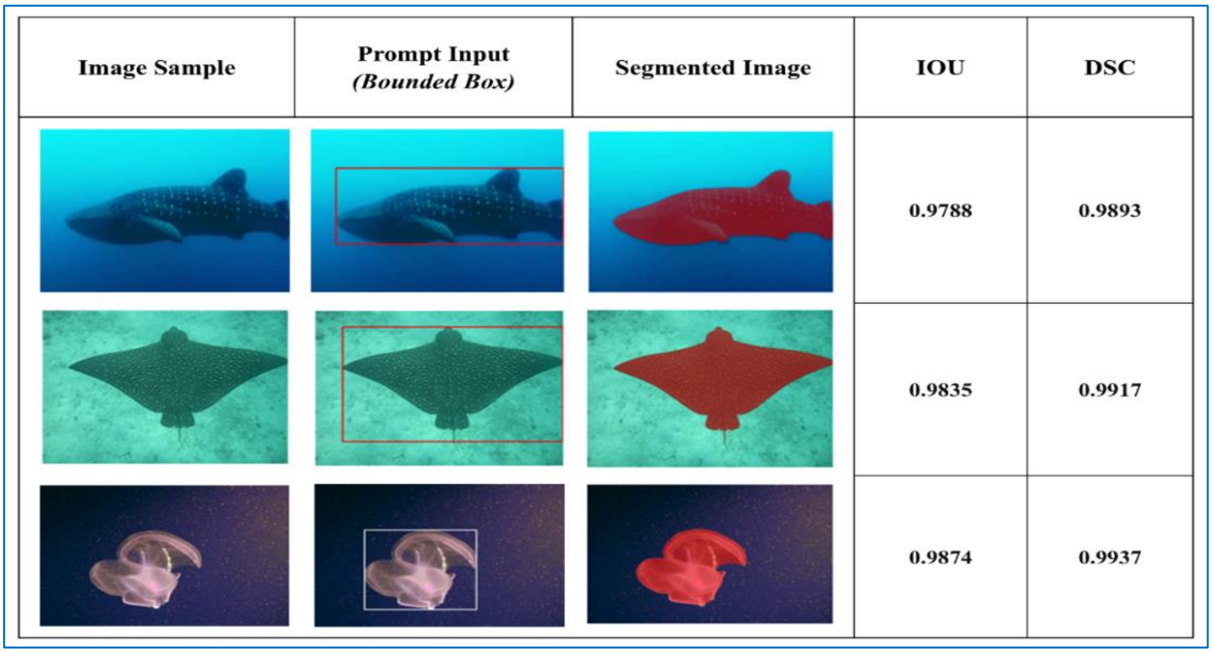

Figure 3. The model SAM segmented underwater images and their respective IoU and DSC scores

International Journal of Applied Mathematics
Volume 38 No. 7s, 2025
ISSN: 1311-1728 (printed version); ISSN: 1314-8060 (on-line version)

The architecture consists of three main components: an image encoder (ViT-based), a prompt encoder (handling points, boxes, or text), and a mask decoder. The image encoder generates a global embedding, while the prompt encoder converts user cues into tokens that guide region-specific segmentation [47],[48]. These tokens are passed into a transformer-based decoder that performs self-attention, cross-attention with image embeddings, and token refinement via MLP layers [49],[50]. The final mask is obtained through a spatial interaction between image features and prompt embeddings. By default, SAM predicts three candidate masks per input to handle segmentation ambiguity and ensure robustness, particularly in visually degraded environments like underwater scenes.

6. Results And Discussion

6.1 The Proposed Model Outcomes

To evaluate the effectiveness of the proposed approach, we selected 50 challenging underwater images from various datasets, including SUIM, NAUTEC UWI Real, and EUVP. Figure 4 displays representative degraded images used for testing. Table 2 summarizes the segmentation results using the SAM model in combination with various enhancement techniques. The metrics include Mean Intersection over Union (mIoU), DSC, and HD95.

Figure 4. Samples of degraded underwater images selected for testing.

Table 2. Segmentation results of 50 images from different datasets tested on a segmentation model with varying methods of enhancement as a preprocessing step.

Model Name	mIoU	% Increase in mIoU	Mean DSC	% Increase in Mean DSC	Mean HD95	% Improve in Mean HD95
SAM	0.8750	NA	0.9275	NA	22.11	NA
CLAHE +SAM	0.8778	+0.3138	0.9298	+0.2465	21.36	3.4820

Received: August 08, 2025

Volume 38 No. 7s, 2025
ISSN: 1311-1728 (printed version); ISSN: 1314-8060 (on-line version)

Color Fusion +SAM	0.8724	-0.2957	0.9248	-0.2961	27.46	-19.4911
GC +SAM	0.8710	-0.4634	0.9245	-0.3237	23.60	-6.3296
HE +SAM	0.8718	-0.3703	0.9251	-0.2548	24.86	-11.0595
HFM +SAM	0.8792	+0.4769	0.9313	+0.4060	21.23	4.1427
ICM +SAM	0.8723	-0.3148	0.9255	-0.2199	22.63	-2.3310
PCDE +SAM	0.8572	-2.0370	0.9163	-1.2037	26.20	-15.6262
Rayleigh's Distribution +SAM	0.8651	-1.1352	0.9218	-0.6160	29.73	-25.6322
RGHS +SAM	0.8744	-0.0767	0.9283	+0.0832	21.50	2.8091
UCM +SAM	0.8705	-0.5217	0.9247	-0.2989	20.66	6.9824
WWPE+SAM	0.8789	+0.4419	0.9309	+0.3659	23.47	-5.8088
Proposed Model	**0.8862**	**+1.2752**	**0.9368**	**+1.0002**	**19.95**	**10.8203**

- From the Table 2, the proposed model achieved the highest segmentation accuracy across all metrics: mIoU: 0.8862 (+1.27% improvement over SAM alone)
- DSC: 0.9368 (+1.00%)
- HD95: 19.95 (10.82% reduction in boundary error)

Other methods like HFM+SAM and WWPE+SAM also offered marginal improvements. In contrast, several techniques (e.g., Color Fusion, PCDE, Rayleigh Stretching) underperformed, likely due to enhancement-induced noise or distortion. Figure 5 illustrates how some methods over sharpen or lose edge fidelity, impacting segmentation quality

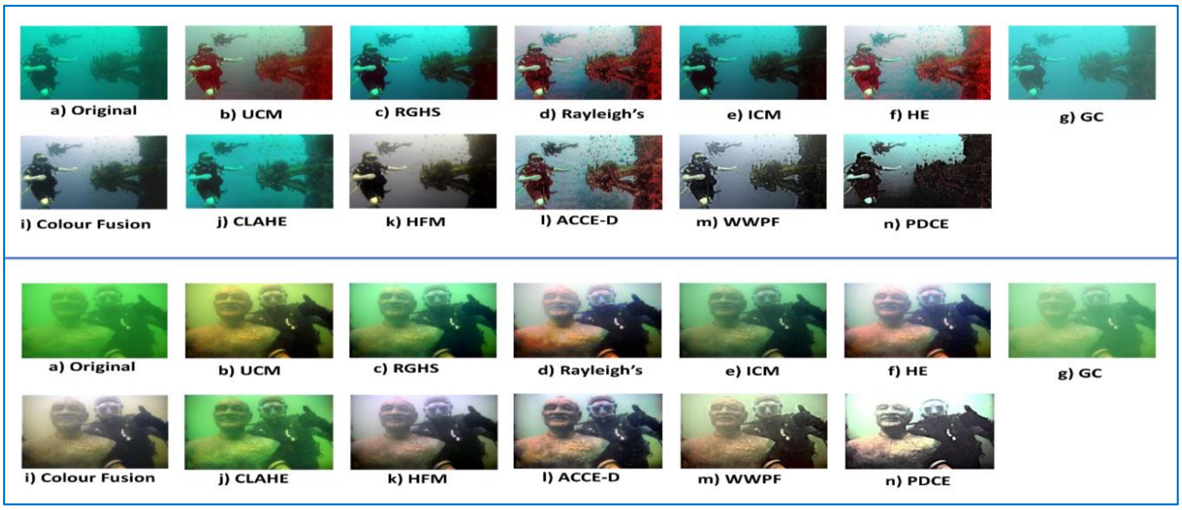

Figure 5. Sample images from the SUIM and NAUTEC UWI Real datasets illustrating the results of various underwater image enhancement methods evaluated in this study.

International Journal of Applied Mathematics
Volume 38 No. 7s, 2025
ISSN: 1311-1728 (printed version); ISSN: 1314-8060 (on-line version)

6.2 Visual Assessment of Segmentation Masks

Figures 6–8 show qualitative segmentation results from SUIM, NAUTEC UWI Real, and EUVP datasets. Visually, the proposed model aligns closely with the ground truth, preserving object boundaries and minimizing segmentation gaps. SAM variants and other models showed less consistent results across images with varying illumination, turbidity, or contrast. Despite the visual similarity between outputs, metric-based comparisons reveal the proposed method maintains stable IoU values, indicating robustness across diverse scenes.

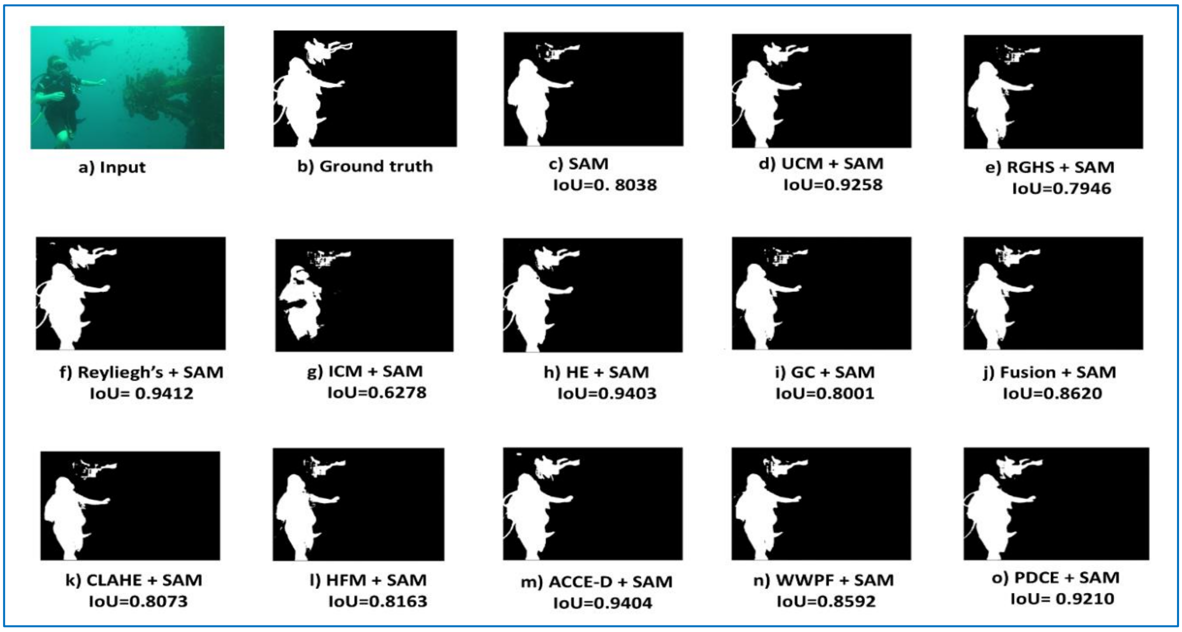

Figure 6. Segmentation results and their respective IoU scores for an Image chosen from SUIM dataset.

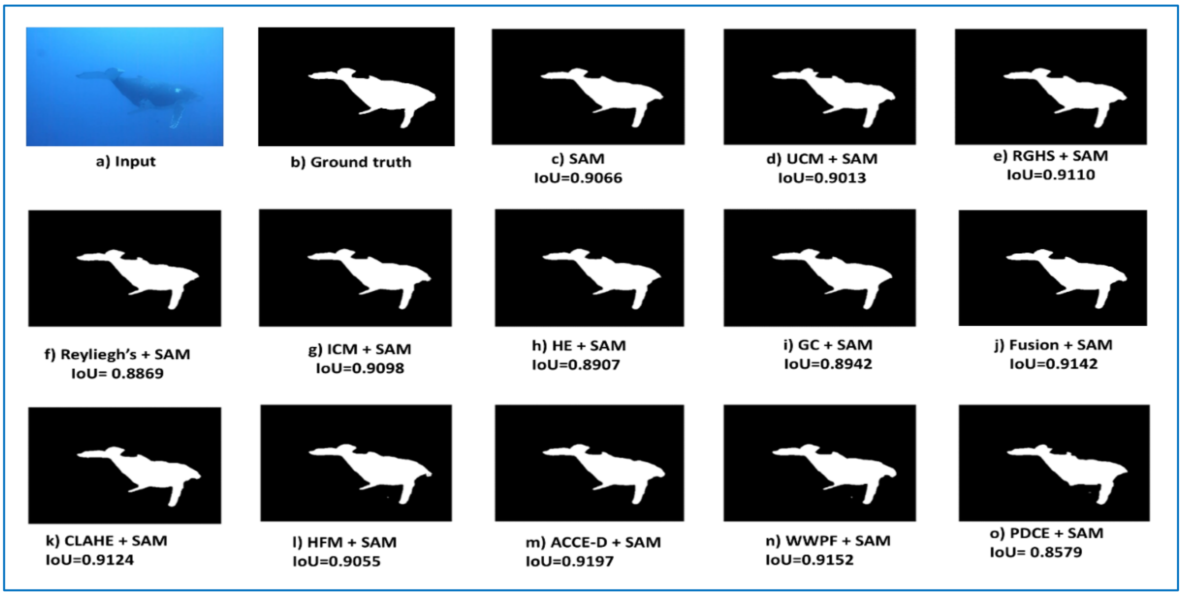

Figure 7. Segmentation results and their respective IoU scores for an Image chosen from NAUTEC UWI Real dataset.

International Journal of Applied Mathematics
Volume 38 No. 7s, 2025
ISSN: 1311-1728 (printed version); ISSN: 1314-8060 (on-line version)

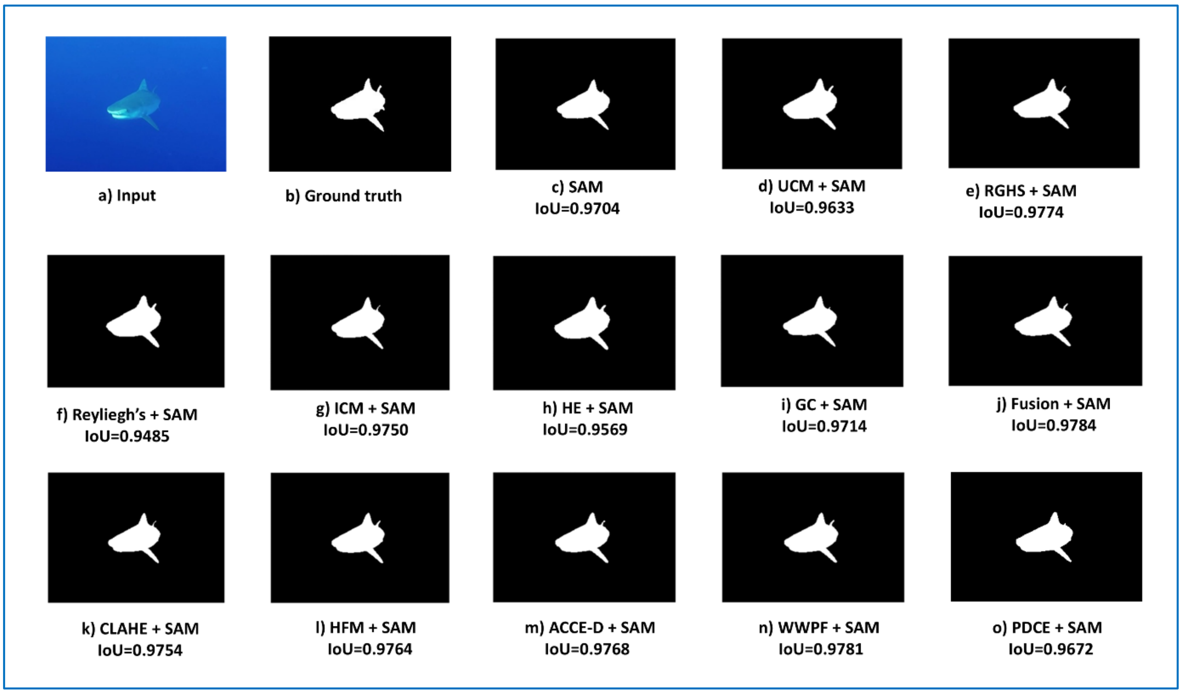

Figure 8. Segmentation results and their respective IoU scores for an image chosen from the EUVP dataset.

6.3 Comparative Evaluation with SOTA Models

To benchmark the model further, we tested 110 underwater images from the SUIM dataset, evaluating segmentation performance across seven object classes: Fishes and Vertebrates (FV), Wrecks (WR), Reefs and Invertebrates (RI), Human Diver (HD), Aquatic Plants (PF), Robots (RO), and Sand-floor/Rocks (SR). As shown in Table 3, the proposed model achieved the highest overall mIoU (0.8126), outperforming even advanced models like SAM2 (0.8050) and EfficientSAM (0.8033). The model consistently delivered high performance across categories, particularly excelling in HD, RO, and FV classes.

Table 3. The segmentation results of various SOTA deep learning models tested on SUIM dataset.

Model Name	mIoU of Different Image Classes							Overall
	HD	PF	WR	RO	RI	FV	SR	mIoU
U-Net	0.3225	0.2185	0.3394	0.2365	0.5028	0.3816	0.4216	0.3461
U-Net (ResNet)	0.7253	0.2370	0.6265	0.5919	0.6993	0.7313	0.6931	0.5844
U-Net (VGG)	0.7900	0.4000	0.6200	0.5100	0.7100	0.7400	0.6800	0.5843
SegNet	0.4567	0.1745	0.3224	0.5572	0.4762	0.4392	0.5151	0.4202
SUIMNet	0.6345	0.2327	0.4125	0.6089	0.5312	0.4602	0.5712	0.4930
PSPNet	0.6504	0.2854	0.4656	0.6289	0.5518	0.4678	0.5598	0.5157
Deeplab	0.5026	0.1705	0.4333	0.6360	0.5718	0.4356	0.5535	0.4719

International Journal of Applied Mathematics
Volume 38 No. 7s, 2025
ISSN: 1311-1728 (printed version); ISSN: 1314-8060 (on-line version)

LEDNet	0.5847	0.1802	0.4286	0.5096	0.5813	0.4613	0.5499	0.4708
BiseNetv2	0.5929	0.1827	0.3958	0.5654	0.5816	0.4733	0.5693	0.4801
UISS-Net	0.8703	0.2948	0.7127	0.8411	0.7070	0.7944	0.6754	0.6994
SAM	0.8804	0.7520	0.7586	0.8515	0.8078	0.7884	0.8219	0.8087
SAM2	0.8936	0.7220	0.7961	0.8739	0.7488	0.7786	0.8218	0.8050
Efficient SAM	0.8842	0.7341	0.7741	0.8375	0.7816	0.7954	0.8159	0.8033
Proposed Model	0.8999	0.7481	0.7629	0.8574	0.8030	0.7955	0.8213	**0.8126**

6.4 Ablation Study: Contribution of Enhancement Components

To evaluate the contribution of individual components within the proposed ACCE-D enhancement pipeline, we conducted ablation experiments by selectively modifying or removing certain key modules. Figure 9 illustrates the ablation setup used to isolate each component's impact on segmentation accuracy using the SAM model.

We analysed the following configurations:

a) DoG + SAM: High-frequency sharpening only.

b) DoG + Soft Thresholding + SAM: Denoising on high-frequency branch.

c) Bilateral + SAM: Low-frequency smoothing only.

d) Bilateral + ACCE + SAM: Contrast and exposure enhancement on low-frequency branch.

e) Denoising +SAM: Few denoising methods implemented individually and in combined form to remove salt-and-pepper and Gaussian noise.

f) Proposed Model: Full pipeline with both enhancement branches integrated (refer figure 1).

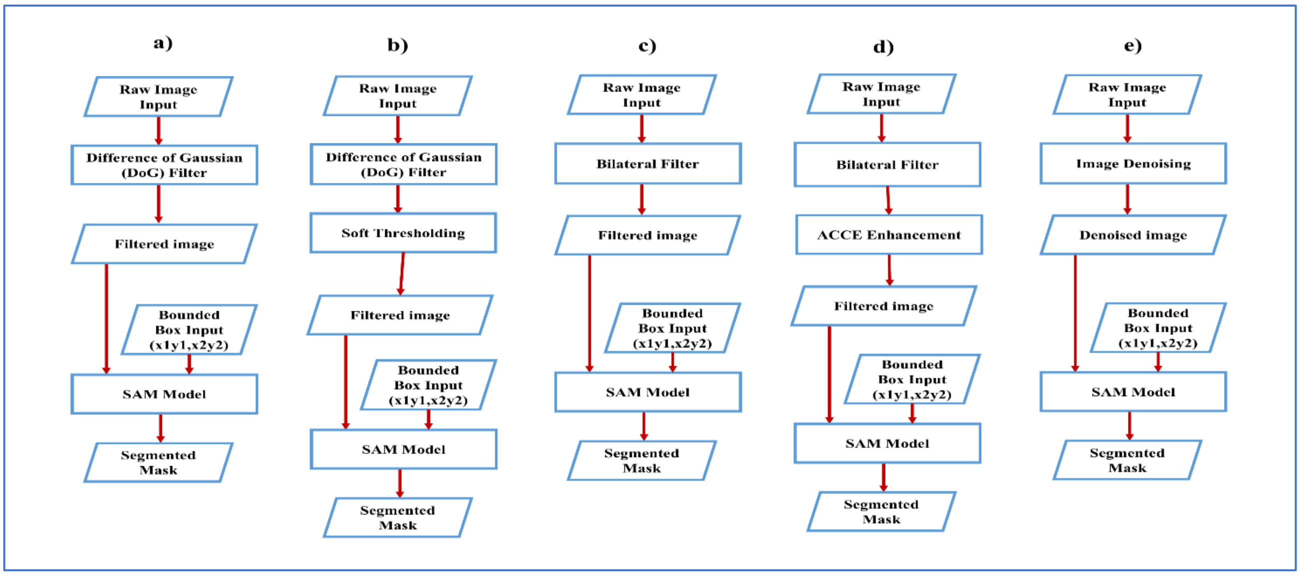

Figure 9. An ablation experimental model to study the impact of different components of the proposed model on segmentation accuracy.

ISSN: 1311-1728 (printed version); ISSN: 1314-8060 (on-line version)

To evaluate the contribution of individual components within the proposed enhancement pipeline, an ablation study was performed using 50 underwater images from multiple datasets. Referring to the Table 4, the baseline SAM model, without any enhancement, achieved an mIoU of 0.8750 and a mean DSC of 0.9275. When tested individually, the DoG filter and the Bilateral filter yielded slightly lower performance than the baseline, with mIoU scores of 0.8602 and 0.8568, respectively. This indicates that while each filter enhances certain image features, their isolated application may introduce artifacts or fail to preserve semantic boundaries critical for segmentation.

Combining DoG with soft thresholding marginally improved results (mIoU: 0.8621, DSC: 0.9169), showing better noise suppression and edge clarity. A further improvement was observed when Bilateral filtering was followed by ACCE processing, achieving an mIoU of 0.8659 and DSC of 0.9194, suggesting that adaptive contrast enhancement complements structural filtering. The complete proposed model, which integrates frequency-aware filtering (DoG + Bilateral), soft thresholding, and adaptive contrast enhancement (ACCE-D), outperformed all other configurations, achieving an mIoU of 0.8862 and a DSC of 0.9368. This validates that the synergistic effect of combining these components leads to more informative input images for segmentation, ultimately improving mask accuracy in underwater scenarios.

Table 4. Segmentation results on 50 images from multiple datasets, evaluating the impact of individual components of the proposed enhancement model.

MODEL	mIoU	Mean DSC
SAM	0.8750	0.9275
DOG+SAM	0.8602	0.9156
DOG+Soft Thresholding+SAM	0.8621	0.9169
Bilateral +SAM	0.8568	0.9139
Bilateral+ACCE+SAM	0.8659	0.9194
Proposed Model	**0.8862**	**0.9368**

To evaluate the impact of various denoising strategies on segmentation accuracy—although denoising was not included in the originally proposed model—several configurations were tested by replacing enhancement methods with individual denoising techniques and applying them with the SAM model. As shown in Table 5, among all tested variants, BM3D + SAM yielded the highest performance, with a mean Intersection over Union (mIoU) of 0.8838 and a mean Dice Similarity Coefficient (DSC) of 0.9341. This demonstrates the effectiveness of BM3D in preserving fine structures and textures relevant to segmentation. Comparable results were observed for AMF + SAM and MF + SAM, indicating that median-based filters are effective in mitigating salt-and-pepper noise.

Wavelet-based methods, such as VisuShrink and BayesShrink, along with Non-Local Means (NLM), also improved segmentation performance by effectively reducing Gaussian noise compared to the baseline SAM model, albeit to a slightly lesser extent. Total Variation (TV) denoising, while still better than the unenhanced baseline in terms of DSC, showed the least improvement among the

ISSN: 1311-1728 (printed version); ISSN: 1314-8060 (on-line version)

tested methods. These results demonstrate that incorporating robust denoising methods prior to segmentation can lead to measurable performance gains, with BM3D standing out as the most effective among the tested techniques.

Table 5. Segmentation results of 50 images from different datasets on denoising based segmentation models.

Model Name	mIoU Result	Mean DSC
SAM	0.8750	0.9275
MF +SAM	0.8819	0.9327
AMF+SAM	0.8827	0.9333
BM3D +SAM	**0.8838**	**0.9341**
Wavelet (visushrink) +SAM	0.8807	0.9319
Wavelet (Bayeshrink) +SAM	0.8821	0.9329
NLM +SAM	0.8806	0.9320
TV +SAM	0.8783	0.9306

We also tested combined filtering approaches (e.g., AMF + BM3D, AMF + NLM) for both salt-and-pepper and Gaussian noise. As presented in Table 6, none of these hybrid denoising strategies surpassed the performance of the proposed model. The results presented in Table 6 show that none of these denoising methods improved the segmentation accuracy. Most denoising methods resulted in the loss of edge details; even edge-preserving denoising methods did not produce beneficial results. Combining image denoising and enhancement processes decreases accuracy compared to the original image segmentation result. Therefore, this strategy is not further discussed.

Table 6. The combined Salt-Pepper and Gaussian filtered segmentation results.

Model Name	mIoU Result	Mean DSC
SAM	0.8750	0.9275
AMF_BM3D +SAM	**0.8821**	**0.9333**
AMF_Wavelet (visushrink) +SAM	0.8763	0.9292
AMF_Wavelet (Bayeshrink)+SAM	0.8790	0.9312
AMF_NLM+SAM	0.8793	0.9312
AMF_TV+SAM	0.8767	0.9296

6.5 Implementation Details

All experiments were performed using MATLAB and Python. The SAM model was executed on Google Colab with T4 GPU (CUDA 12.2), 15 GB GPU RAM, and 12 GB CPU RAM.

6.6 Computational Efficiency and Deployment Considerations

The proposed framework achieves an average processing speed of 2.91511 seconds per frame (≈0.34 FPS) on the test hardware. Although this is insufficient for continuous frame-by-frame segmentation during high-speed navigation, it is acceptable for underwater inspection and analysis tasks, where segmentation is applied selectively to frames of interest rather than entire video streams.

In practical ROV/AUV deployments, high-frequency object detection modules are used for real-time navigation, while segmentation is applied intermittently for mapping, monitoring, or post-mission analysis. Under this operational paradigm, the observed runtime is reasonable. Further optimization (e.g., mixed-precision inference, model pruning/quantization, or ONNX/TensorRT conversion) can improve throughput if required for real-time applications.

Summary of Findings:

- The proposed model significantly improves segmentation accuracy on degraded underwater images.
- It outperforms traditional enhancement methods and even advanced segmentation models like SAM2 and EfficientSAM.
- Ablation studies confirm that both high- and low-frequency enhancement components are critical to performance.
- Denoising methods alone or in combination do not yield better results, often harming edge preservation.

7. conclusion

This study proposed a hybridized deep learning model that integrates an adaptive image enhancement method with the Segment Anything Model to improve underwater image segmentation. The model demonstrated robust performance across diverse datasets, outperforming several state-of-the-art methods in terms of mIoU, Dice score, and boundary precision. The ablation study confirmed that both high- and low-frequency enhancement components significantly contribute to segmentation quality, while traditional denoising techniques often remove essential edge details and degrade performance. Notably, the proposed model generalizes well even without domain-specific training, making it suitable for low-data or zero-shot scenarios. However, certain limitations remain. In complex underwater scenes affected by turbidity, uneven lighting, or occlusion, segmentation performance showed some decline—highlighting the challenge of using static enhancement parameters and prompt-based segmentation under highly variable conditions. Future work may explore adaptive enhancement modules and automated prompt strategies to improve robustness in such scenarios. These findings reinforce that segmentation quality in underwater imagery is more strongly influenced by the clarity and contrast of input data than by changes in segmentation architecture alone, emphasizing the critical role of enhancement-aware preprocessing.

ACKNOWLEDGMENTS

NOT APPLICABLE.

FUNDING INFORMATION

No funding received for this research.

AUTHOR CONTRIBUTIONS STATEMENT

Name of Author	C	M	So	Va	Fo	I	R	D	O	E	Vi	Su	P	Fu
Abhisheka Thumbesara Eshwara	✓	✓	✓	✓	✓	✓	✓	✓	✓	✓			✓	
Basavaraj Ningappa Jagadale		✓				✓	✓	✓	✓	✓	✓	✓		
Madhuri Gurram Ramesh				✓		✓			✓		✓		✓	
Chandrakantha Tholalemane Satyanarayana					✓		✓				✓			

C : **C**onceptualization	I : **I**nvestigation	Vi : **Vi**sualization
M : **M**ethodology	R : **R**esources	Su : **Su**pervision
So : **So**ftware	D : **D**ata Curation	P : **P**roject administration
Va: **Va**lidation	O : Writing - **O**riginal Draft	Fu : **Fu**nding acquisition
Fo : **Fo**mal analysis	E : Writing - Review & **E**diting	

CONFLICT OF INTEREST STATEMENT

The authors declare that they have no conflict of interest.

INFORMED CONSENT

Not Applicable

ETHICAL APPROVAL

Not Applicable

DATA AVAILABILITY STATEMENT

We have used three datasets for this study. These datasets are publicly available in the flowing IP addresses.

SUIM Dataset: https://github.com/xahidbuffon/SUIM

NAUTEC Underwater Real dataset: https://1drv.ms/f/s!ApAbq4UfbfzjhzE6ttiTtxdpMg9i

ISSN: 1311-1728 (printed version); ISSN: 1314-8060 (on-line version)

EUVP dataset: https://irvlab.cs.umn.edu/resources/euvp-dataset

The base code for the SAM model is available publicly at GitHub repository by the SAM author https://github.com/facebookresearch/segment-anything

References

[1] Jian, M., Liu, X., Luo, H., Lu, X., Yu, H., & Dong, J. (2021). Underwater image processing and analysis: A review. *Signal Processing: Image Communication*, *91*, 116088. https://doi.org/10.1016/j.image.2020.116088

[2] Drews-Jr, P., Souza, I. de, Maurell, I. P., Protas, E. V., & C. Botelho, S. S. (2021). Underwater image segmentation in the wild using deep learning. Journal of the Brazilian Computer Society, 27(1), 12. https://doi.org/10.1186/s13173-021-00117-7

[3] Fabic, J. N., Turla, I. E., Capacillo, J. A., David, L. T., & Naval, P. C. (2013). Fish population estimation and species classification from underwater video sequences using blob counting and shape analysis. *2013 IEEE International Underwater Technology Symposium (UT)*, 1–6. https://doi.org/10.1109/UT.2013.6519876

[4] Martin-Abadal, M., Ruiz-Frau, A., Hinz, H., & Gonzalez-Cid, Y. (2020). *The Application of Deep Learning in Marine Sciences* (pp. 193–230). https://doi.org/10.1007/978-3-030-31760-7_7

[5] Wenjuan, M., & Feng, X. (2021). RETRACTED ARTICLE: Underwater image segmentation based on computer vision and research on recognition algorithm. Arabian Journal of Geosciences, 14(18), 1836. https://doi.org/10.1007/s12517-021-08081-4

[6] Sanz, P. J., Vincze, M., & Fornas, D. (2017). Increasing underwater manipulation autonomy using segmentation and visual tracking. OCEANS 2017 - Aberdeen, 1–5. https://doi.org/10.1109/OCEANSE.2017.8084762

[7] Wei, L., Kong, S., Wu, Y., & Yu, J. (2022). Image Semantic Segmentation of Underwater Garbage with Modified U-Net Architecture Model. Sensors, 22(17), 6546. https://doi.org/10.3390/s22176546

[8] Kirillov, A., Mintun, E., Ravi, N., Mao, H., Rolland, C., Gustafson, L., Xiao, T., Whitehead, S., Berg, A. C., Lo, W.-Y., Dollár, P., & Girshick, R. (2023). Segment Anything. ArXiv. https://doi.org/10.48550/arXiv.2304.02643

[9] Minaee, S., Boykov, Y. Y., Porikli, F., Plaza, A. J., Kehtarnavaz, N., & Terzopoulos, D. (2021). Image Segmentation Using Deep Learning: A Survey. IEEE Transactions on Pattern Analysis and Machine Intelligence, 1–1. https://doi.org/10.1109/TPAMI.2021.3059968

[10] Zhang, H., Zhang, S., Wang, Y., Liu, Y., Yang, Y., Zhou, T., & Bian, H. (2021). Subsea pipeline leak inspection by autonomous underwater vehicle. Applied Ocean Research, 107, 102321. https://doi.org/10.1016/j.apor.2020.102321

[11] Donaldson, J. A., Drews Jr, P., Bradley, M., Morgan, D. L., Baker, R., & Ebner, B. C. (2020). Countering low visibility in video survey of an estuarine fish assemblage. Pacific Conservation Biology, 26(2), 190. https://doi.org/10.1071/PC19019

[12] Zhang, L., Qiu, Y., Fan, J., Li, S., Hu, Q., Xing, B., & Xu, J. (2024). Underwater fish detection and counting using image segmentation. Aquaculture International, 32(4), 4799–4817. https://doi.org/10.1007/s10499-024-01402-w

[13] Liu, F., & Fang, M. (2020). Semantic Segmentation of Underwater Images Based on Improved Deeplab. Journal of Marine Science and Engineering, 8(3), 188. https://doi.org/10.3390/jmse8030188

[14] Kumar Rai, R., Gour, P., & Singh, B. (2012). Underwater Image Segmentation using CLAHE Enhancement and Thresholding. International Journal of Emerging Technology and Advanced Engineering, 2(1), 118–123. www.ijetae.com

[15] Iqbal, K., Odetayo, M., James, A., Rosalina Abdul Salam, & Abdullah Zawawi Hj Talib. (2010). Enhancing the low quality images using Unsupervised Colour Correction Method. 2010 IEEE International Conference on Systems, Man and Cybernetics, 1703–1709. https://doi.org/10.1109/ICSMC.2010.5642311

[16] Huang, D., Wang, Y., Song, W., Sequeira, J., & Mavromatis, S. (2018). Shallow-Water Image Enhancement Using Relative Global Histogram Stretching Based on Adaptive Parameter Acquisition. In MultiMedia Modeling (Vol. 10704, pp. 453–465). Springer, Cham. https://doi.org/10.1007/978-3-319-73603-7_37

[17] Xie, Y., Ning, L., Wang, M., & Li, C. (2019). Image Enhancement Based on Histogram Equalization. Journal of Physics: Conference Series, 1314(1). https://doi.org/10.1088/1742-6596/1314/1/012161

[18] Iqbal, K., Abdul salam, R., & osman, A. (2007). Underwater Image Enhancement Using an Integrated Colour Model. IAENG International Journal of Computer Science, 34(2), 12. https://www.researchgate.net/profile/Rosalina-Abdul-Salam/publication/26587242_Underwater_Image_Enhancement_Using_an_Integrated_Colour_Model/links/658e3af20bb2c7472b183627/Underwater-Image-Enhancement-Using-an-Integrated-Colour

[19] Abdul Ghani Ahmad Shahrizan, & Nor Ashidi Mat Isa. (2014). Underwater image quality enhancement through composition of dual-intensity images and Rayleigh-stretching. SpringerPlus, 3(1), 757. https://doi.org/10.1186/2193-1801-3-757

[20] Amiri, S. A., & Hassanpour, H. (2012). A Preprocessing Approach for Image Analysis Using Gamma Correction. International Journal of Computer Applications, 38(12), 975–8887. https://research.ijcaonline.org/volume38/number12/pxc3876914.pdf

[21] Ancuti, C., Ancuti, C. O., Haber, T., & Bekaert, P. (2012). Enhancing underwater images and videos by fusion. 2012 IEEE Conference on Computer Vision and Pattern Recognition, 81–88. https://doi.org/10.1109/CVPR.2012.6247661

[22] An, S., Xu, L., Deng, Z., & Zhang, H. (2024). HFM: A hybrid fusion method for underwater image enhancement. Engineering Applications of Artificial Intelligence, 127, 107219. https://doi.org/10.1016/j.engappai.2023.107219

[23] Li, X., Hou, G., Li, K., & Pan, Z. (2022). Enhancing underwater image via adaptive color and

ISSN: 1311-1728 (printed version); ISSN: 1314-8060 (on-line version)

contrast enhancement, and denoising. *Engineering Applications of Artificial Intelligence*, *111*, 104759. https://doi.org/10.1016/j.engappai.2022.104759

[24] Zhang, W., Zhou, L., Zhuang, P., Li, G., Pan, X., Zhao, W., & Li, C. (2024). Underwater Image Enhancement via Weighted Wavelet Visual Perception Fusion. IEEE Transactions on Circuits and Systems for Video Technology, 34(4), 2469–2483. https://doi.org/10.1109/TCSVT.2023.3299314

[25] Tolstikhin, I., Houlsby, N., Kolesnikov, A., Beyer, L., Zhai, X., Unterthiner, T., Yung, J., Steiner, A., Keysers, D., Uszkoreit, J., Lucic, M., & Dosovitskiy, A. (2021). MLP-Mixer: An all-MLP Architecture for Vision. ArXiv. https://doi.org/10.48550/arXiv.2104.09917

[26] Badrinarayanan, V., Kendall, A., & Cipolla, R. (2017). SegNet: A Deep Convolutional Encoder-Decoder Architecture for Image Segmentation. IEEE Transactions on Pattern Analysis and Machine Intelligence, 39(12), 2481–2495. https://doi.org/10.1109/TPAMI.2016.2644615

[27] O'Byrne, M., Pakrashi, V., Schoefs, F., & Ghosh, B. (2018). Semantic Segmentation of Underwater Imagery Using Deep Networks Trained on Synthetic Imagery. Journal of Marine Science and Engineering, 6(3), 93. https://doi.org/10.3390/jmse6030093

[28] Fan, X., Cao, P., Shi, P., Chen, X., Zhou, X., & Gong, Q. (2022). An underwater dam crack image segmentation method based on multi-level adversarial transfer learning. Neurocomputing, 505, 19–29. https://doi.org/10.1016/j.neucom.2022.07.036

[29] Alshdaifat, N. F. F., Talib, A. Z., & Osman, M. A. (2020). Improved deep learning framework for fish segmentation in underwater videos. Ecological Informatics, 59, 101121. https://doi.org/10.1016/j.ecoinf.2020.101121

[30] Deng, R., Zhao, L., Li, H., & Liu, H. (2023). Cformer: An underwater image enhancement hybrid network combining convolution and transformer. IET Image Processing, 17(13), 3841–3855. https://doi.org/10.1049/ipr2.12901

[31] Chen, L., Jiang, Z., Tong, L., Liu, Z., Zhao, A., Zhang, Q., Dong, J., & Zhou, H. (2020, August 21). Perceptual underwater image enhancement with deep learning and physical priors. arXiv.org. https://arxiv.org/abs/2008.09697

[32] Qian, J., Li, H., & Zhang, B. (2024). HA-Net: a hybrid algorithm model for underwater image color restoration and texture enhancement. Electronics, 13(13), 2623. https://doi.org/10.3390/electronics13132623

[33] Ronneberger, O., Fischer, P., & Brox, T. (2015). U-NET: Convolutional Networks for Biomedical Image Segmentation. arXiv (Cornell University). https://doi.org/10.48550/arxiv.1505.04597

[34] Salas-Espinales, A., Vélez-Chávez, E., Vázquez-Martín, R., García-Cerezo, A., & Mandow, A. (2024). U-Net/ResNet-50 Network with Transfer Learning for Semantic Segmentation in Search and Rescue. In Lecture notes in networks and systems (pp. 244–255). https://doi.org/10.1007/978-3-031-59167-9_21

[35] Pravitasari, A. A., Iriawan, N., Almuhayar, M., Azmi, T., Irhamah, I., Fithriasari, K., Purnami, S. W., & Ferriastuti, W. (2020). UNet-VGG16 with transfer learning for MRI-based brain tumor segmentation. TELKOMNIKA (Telecommunication Computing Electronics and Control), 18(3),

1310. https://doi.org/10.12928/telkomnika.v18i3.14753

[36] Badrinarayanan, V., Handa, A., & Cipolla, R. (2015). SEGNet: a deep convolutional Encoder-Decoder architecture for robust semantic Pixel-Wise labelling. arXiv (Cornell University). https://doi.org/10.48550/arxiv.1505.07293

[37] Islam, M. J., Edge, C., Xiao, Y., Luo, P., Mehtaz, M., Morse, C., Enan, S. S., & Sattar, J. (2020). Semantic Segmentation of Underwater Imagery: Dataset and benchmark. 2021 IEEE/RSJ International Conference on Intelligent Robots and Systems (IROS), 1769–1776. https://doi.org/10.1109/iros45743.2020.9340821

[38] Yu, C., Gao, C., Wang, J., Yu, G., Shen, C., & Sang, N. (2021). BiSeNet V2: Bilateral Network with Guided Aggregation for Real-Time Semantic Segmentation. International Journal of Computer Vision, 129(11), 3051–3068. https://doi.org/10.1007/s11263-021-01515-2

[39] Zhao, H., Shi, J., Qi, X., Wang, X., & Jia, J. (2016). Pyramid Scene Parsing network. arXiv (Cornell University). https://doi.org/10.48550/arxiv.1612.01105

[40] He, Z., Cao, L., Luo, J., Xu, X., Tang, J., Xu, J., Xu, G., & Chen, Z. (2024). UISS-Net: Underwater Image Semantic Segmentation Network for improving boundary segmentation accuracy of underwater images. Aquaculture International, 32(5), 5625–5638. https://doi.org/10.1007/s10499-024-01439-x

[41] Chen, L., Papandreou, G., Kokkinos, I., Murphy, K., & Yuille, A. L. (2017b). DeepLab: Semantic Image Segmentation with Deep Convolutional Nets, Atrous Convolution, and Fully Connected CRFs. IEEE Transactions on Pattern Analysis and Machine Intelligence, 40(4), 834–848. https://doi.org/10.1109/tpami.2017.2699184

[42] Wang, Y., Zhou, Q., Liu, J., Xiong, J., Gao, G., Wu, X., & Latecki, L. J. (2019). LEDNET: a lightweight Encoder-Decoder network for Real-Time semantic segmentation. 2022 IEEE International Conference on Image Processing (ICIP), 1860–1864. https://doi.org/10.1109/icip.2019.8803154

[43] Ravi, N., Gabeur, V., Hu, Y., Hu, R., Ryali, C., Ma, T., Khedr, H., Rädle, R., Rolland, C., Gustafson, L., Mintun, E., Pan, J., Alwala, K. V., Carion, N., Wu, C., Girshick, R., Dollár, P., & Feichtenhofer, C. (2024). SAM 2: Segment anything in images and videos. arXiv (Cornell University). https://doi.org/10.48550/arxiv.2408.00714

[44] Xiong, Y., Varadarajan, B., Wu, L., Xiang, X., Xiao, F., Zhu, C., Dai, X., Wang, D., Sun, F., Iandola, F., Krishnamoorthi, R., & Chandra, V. (2023). EFficientSAM: Leveraged Masked Image Pretraining for efficient Segment anything. arXiv (Cornell University). https://doi.org/10.48550/arxiv.2312.00863

[45] Girshick, R., Donahue, J., Darrell, T., & Malik, J. (n.d.). Rich feature hierarchies for accurate object detection and semantic segmentation Tech report (v5). ArXiv. Retrieved 10 September 2024, from https://doi.org/10.48550/arXiv.1311.2524

[46] Brown, T. B., Mann, B., Ryder, N., Subbiah, M., Kaplan, J., Dhariwal, P., Neelakantan, A., Shyam, P., Sastry, G., Askell, A., Agarwal, S., Herbert-Voss, A., Krueger, G., Henighan, T., Child,

ISSN: 1311-1728 (printed version); ISSN: 1314-8060 (on-line version)

R., Ramesh, A., Ziegler, D. M., Wu, J., Winter, C., … Amodei, D. (2020). Language Models are Few-Shot Learners. ArXiv. https://doi.org/10.48550/arXiv.2005.14165

[47] Xu, N., Price, B., Cohen, S., Yang, J., & Huang, T. (2016). Deep Interactive Object Selection. 2016 IEEE Conference on Computer Vision and Pattern Recognition (CVPR), 373–381. https://doi.org/10.1109/CVPR.2016.47

[48] Mahadevan, S., Voigtlaender, P., & Leibe, B. (2018). Iteratively Trained Interactive Segmentation. ArXiv. https://doi.org/10.48550/arXiv.1805.04398

[49] Carion, N., Massa, F., Synnaeve, G., Usunier, N., Kirillov, A., & Zagoruyko, S. (2020). End-to-End Object Detection with Transformers. ArXiv. https://doi.org/10.48550 /arXiv.2005.12872

[50] Vaswani, A., Shazeer, N., Parmar, N., Uszkoreit, J., Jones, L., Gomez, A. N., Kaiser, L., & Polosukhin, I. (2017). Attention Is All You Need. ArXiv. https://doi.org/10.48550 /arXiv.1706.03762

BIOGRAPHIES OF AUTHORS

	**Abhisheka Thumbesara Eshwara** is a part time Research scholar at Department of Electronics, Kuvempu University, Shivamogga and Technical Officer at All India Institute of Speech and Hearing (AIISH), Mysuru. He holds Post graduate degree M.Sc in Electronics from Kuvempu University, cleared NET Exam in Electronic Science two times (2014, 2016) conducted by UGC. Cleared K-SET exam in Electronic Science (2013). His area of interest is Digital image processing. He has teaching Experience of 6 years for MSc in Electronics and for Diploma in Hearing aid and Ear Mold Technology. Email: te.abhishek@gmail.com Scopus ID: 57274660500
	**Basavaraj Ningappa Jagadale** is an experienced academician, researcher, and administrator with over 25 years of teaching and 20 years of research experience. He currently serves as the Associate Professor and Chairman of the Department of PG Studies and Research in Electronics at Kuvempu University. With expertise in Digital Signal and Image Processing and Artificial Intelligence, he holds a Ph.D. from Karnatak University, Dharwad. Dr. Jagadale has published 30+ international journal papers, 20+ conference papers, and guided 10 Ph.D. scholars, with four currently under his supervision. He did his post-doctoral research at the University of Pennsylvania, USA (2015-16). Passionate about technological advancements and education, he continues to lead impactful research and mentor young scholars in electronics and communication.

International Journal of Applied Mathematics
Volume 38 No. 7s, 2025
ISSN: 1311-1728 (printed version); ISSN: 1314-8060 (on-line version)

	Email: basujagadale@gmail.com Scopus ID: 35174467000
	**Madhuri Gurram Ramesh** Madhuri G R is an Assistant Professor in the Department of Electronics at Kuvempu University, India. Her Research interest include Microwave Electronics and Digital Image Processing using Machine learning. She has 15 years of teaching experience and 8 years of research experience. She holds a Ph. D from Gulbarga University, Kalburgi and published 15+ Journal articles, 10+ conference papers and actively involved in guiding research students. Currently four scholars are under her supervision. Email: madhurigr12@gmail.com
	**Chandrakantha Tholalemane Satyanarayana** holds an M.Sc. in Electronics from Mangalore University Mangalagangotri, Karnataka, India. and is currently a Lecturer and Research Scholar at Kuvempu University, Karnataka, India. With over five years of academic experience, his research focuses on AI-driven medical image analysis, including brain tumour detection, lung tumour classification, and breast cancer diagnosis, with publications in international journals and conferences. Email: chandrabeluved@gmail.com Scopus ID: 58038743300

Received: August 08, 2025